Evaluation of the Melted Zone Microstructure in the Interface of the Dissimilar Weld between A335 Low Alloy Steel and ER309L Filler Metal by Gas Tungsten Arc Welding

I. Hajiannia [1], M. Shamanian [2], M. Kasiri [3]*
[1,3]Department of Materials Engineering, Najafabad Branch, Islamic Azad University, Najafabad 85141-43131, Iran
[2]Department of Materials Engineering, Isfahan University of Technology, Isfahan 84156-83111, Iran

Abstract

In the present study, the microstructure and mechanical properties of the dissimilar welding between ASTM A335 low alloy steel and ER309L austenitic stainless steel were investigated using the gas tungsten arc welding process. The welding of dissimilar materials between ASTM A335 low alloy steel and ER309L austenitic stainless steel was found to have a significant effect on the microstructure when the filler metal of ER309L was used. This research also studied the effect of carbon migration from the heat-affected zone (HAZ) to the melted zone in the interface between A335 low alloy steel and 309L filler metal using microstructure analysis and Scanning electron microscopy-energy dispersive spectroscopy (SEM-EDS) Line Scan Technique. The results showed that the solidification of 309L as a primary ferrite exhibited a skeletal ferrite morphology and the solidification of ferritic-austenitic (FA) type. Moreover, the results of EDS provided evidence showing carbon migration from the low chromium side to the weld metal which had a higher chromium content and a tiny martensitic zone occurred in the melt boundary with a high hardness value. In the tensile test, all specimens were broken in the HAZ of A335 low alloy base metal with a ductile fracture and the welded specimens also showed the ductile fracture in the impact test.

Keywords: Low alloy steel, Carbon migration, Microstructure, Mechanical properties.

1. Introduction

Chromium-Molybdenum low alloy steels are resistant to erosion and corrosion. ASTM A335 low alloy steel is widely used in many industries such as petrochemicals, electric power plants, and nuclear power plants [1].Cr-Mo low-alloy steels can be employed at high service temperatures with good creep strength. Dissimilar joining is used in different parts of steam generators where the differential temperature is critical. The result of the welding A335 low alloy steel with austenitic stainless steel ER309L filler metal, which can be considered as dissimilar welds between high Cr steels and low Cr steels, is the formation of a carbon migration zone due to the difference in carbon content. In this research, attempts were made to study the effect of welding on the microstructure in different zones of dissimilar joints, as well as the mechanical properties in the dissimilar joining of Cr-Mo low alloy steel between A335 grades P11 and ER309L. The welding of dissimilar metals is efficient if the welding conditions that determine the duration of the interaction between the solid and liquid metal are strictly controlled. The properties of the welded joints and the feasibility of the welding processes are influenced by many factors; for example, carbon migration from the low-alloy side and the microstructure gradient and residual stress situations across different regions of the weld metal can be mentioned. One of the important factors predicting cracking in several passes is controlling the weld metal ferrite content (4-9%). It can be observed that during welding stainless steel to carbon and low-alloy steels, hot cracking may occur due to low melting point impurities, such as phosphor (P) and sulfur (S). Moreover, there is a risk of low-temperature cracking, because of the increase in the dilution of the base metal on the carbon/low-alloy steel side; the weld metal contains a hard martensite phase [2]. In dissimilar welding, one of the most important concerns is the selection of a proper filler material.

** Corresponding author*
Email: Iman_hajiannia@yahoo.com
Address: Department of Materials Engineering, Najafabad Branch, Islamic Azad University, Najafabad 85141-43131, Iran
1. PhD Student
2. Professor
3.Associate Professor

In recent years, some studies on the evaluation of dissimilar welding of stainless steel and low alloy steel have been conducted. Sae-teaw et al. [3], for example, investigated the welding between Cr-Mo Steel grade 9Cr-1Mo and 2.25Cr-1Mo. The results showed that the low carbon side presented the formation of soft zone while the high carbon side led to the formation of a precipitate zone which was $Cr_{23}C_6$. Klueh [4] investigated the failure of a transferred joint between 2.25 Cr-1Mo steel and 321austenitic stainless steel using Ni-based Inconel 182 filler metal. It was illustrated that after heating this joint at high temperatures for 15 to 20 years, the heat-affected zone contained large ferrite grains; hence, cracking happened in this zone. In another study, Falat et al.[5] probed the microstructure and creep characteristics of some dissimilar T91/TP316H martensitic/austenitic welded joint with Ni-based weld metal, realizing that the microstructure of Ni weld metal was very heterogeneous. In addition, the martensitic part of the welded joint showed a wide heat-affected zone (HAZ). Conversely, the HAZ of the austenitic steel was limited to only a narrow region with coarsened polygonal grains. The aim of this study was to investigate the mechanical properties and the microstructure of different welding zones.

2. Experimental Procedure

The base metals used in this study were A335 low alloy steel pipes. The pipes were 8 mm in thickness, 400 mm in length and 200 mm in outer diameter. The filler metal, ER309L, was used to join the base metals. The nominal chemical compositions of the base and filler metals are given in Table 1.

Table 1. The chemical composition of used materials (based on wt. %).

Element	C	Cr	Ni	Mo	Mn	Si	Ti	Cu	Nb	Fe
A335	0.1	1.12	-	0.5	.03	1.0	-	0.08	-	BAL
ER309L	0.02	23.7	13.9	0.04	1.8	0.51	-	0.05	-	BAL

Wires 2.4 mm in diameter were used for root pass and hot and cover passes. Before welding, the pipes were prepared to make a single V groove butt configuration. The welding was done by gas tungsten arc welding process with Direct-Current Electrode Negative (GTAW-DCEN) and argon gas shield of 99.99% purity. The inter-pass temperature was selected to be 150 ^oC in order to minimize the tension of the weld metal solidification 6).The welding parameters and the heat input in each welding pass are given in Table 2.

Table 1. The chemical composition of used materials (based on wt. %).

Filler Metal	Welding Parameters				
	Pass No.	Current (A)	Volt (V)	Welding Speed (mms^{-1})	Heat Input ($kJmm^{-1}$)
ER309L	1	150	12	1.1	0.981
	2	140	10	1.0	0.840
	3	130	11	1.1	0.709
	4	110	12	1.1	0.720

According to ASME SEC.IX [7], two specimens from the weldment metal were selected to evaluate the tensile properties. The tensile test was carried out by an Instron 8055 tensile machine. The elongation ratio, tensile strength and yield strength of specimens were calculated and the impact test specimens with the dimensions of 55mm*10mm*10mm and 2-mm notches with the angle 45^o were prepared based on ASME SEC.IX to compare the impact resistance of the weld metals. The weld metal was placed in the center of the specimens. There were three specimens from weldment in this test. The Charpy impact test was performed on the specimens at -20 ^oC and 27 ^oC using Santum machine, and the absorbed force was reported during the test. The crack surfaces of specimens were evaluated by scanning electron microscopy after the test. Microindention hardness measurement was performed across the welds to obtain the hardness profiles in the weld metal, the heat-affected zone and the base metal at a load of 100g using Buehler microindention hardness tester. In order to study the microstructure of the base metals, weld metals, and the heat-affected zone, the metallography procedure was used [7]. Therefore, for each joint, two specimens with proper size were prepared by grinding using 80 to 2000 grits silicon carbide paper. This was followed by final polishing with 0.3 μm alumina powders. The specimens were etched for 15 sec using Nital solution (2% nitrate acid in alcohol) to show the structure of low alloy steel, and they were also etched by Marbel solution (10 gr of $CuSO_4$ + 50cc HCI + 50cc H_2O) to find the microstructure of austenitic stainless steel weld metal. The (FMP30 Fischer) ferritescope was also used to determine the ferrite and austenitic phase ratios.

3. Results and Discussion

Fig. 1 shows the microstructure of A335 chromium-molybdenum low alloy steel in which ferrite grains with dark pearlite grains can be observed.

The microstructure of 309L austenitic stainless steel weld metal (which was related to the root pass) is shown in Fig. 2.

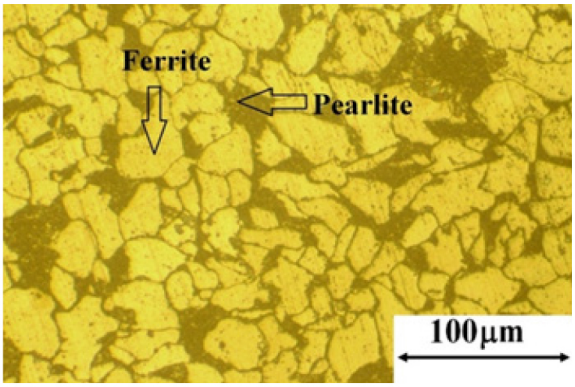

Fig. 1. Optical micrographs of A335 low alloy steel.

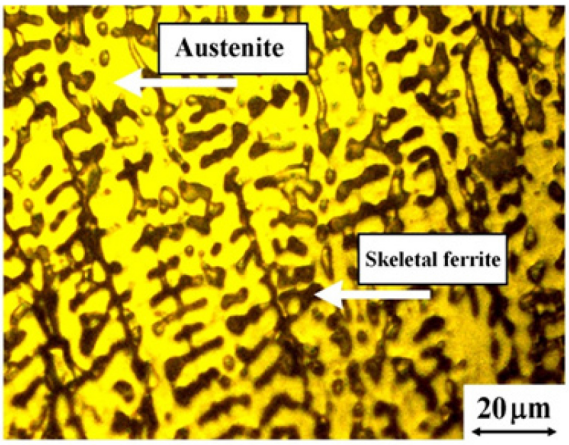

Fig. 2. The microstructure of ER309L weld metal.

The solidification of 309L as a primary ferrite exhibited a skeletal ferrite morphology and the solidification of FA type. The same results were gained by Lippold and Koteki [1] for the solidification of this weld metal. They showed that when the cooling rate of weldment was moderate and/or when the Creq/ Nieq was low, though still in the FA range, a skeletal ferrite morphology was produced. The ferrite content of root pass of 309L filler metal was about 5.7% (by a ferritescope). The interface between A335 low alloy steel base metal and 309L weld metal is presented in Fig. 3.

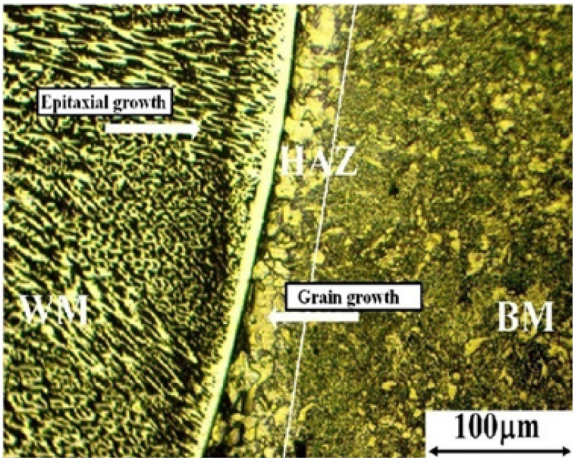

Fig. 3. Interfaces between the 309L weld metal and the A335 base metal.

The figure shows that the grain growth that occurred in the HAZ of low alloy steel was planar [8].Moreover, in the transformation zone, melt boundary was changed impressively in a very short distance. There was a kind of carbon migration from HAZ to the melt zone during the welding because of the change in the chemical composition of A335 which contained more carbon (Quintuple) than 309L weld metal. The information obtained from the tension-strain graphs is given in Table 3.

Table 3. The results of the tension.

Type of filler metal	Yield strength (MPa)	Ultimate tensile strength (MPa)	Elongation (%)	Location of failure
ER309L	444	572	42	HAZ A335

As shown, the carbon migration made a relatively soft ferrite region between the stronger weld metal and the base metal. As mentioned before, grain growth happened at the HAZ of A335 low alloy steel. All these factors could justify the fracture process of specimens at the HAZ of A335 base metal. In Fig. 4, the fractured surface of the tensile specimen has been analyzed using SEM. This fracture surface consisted of uniform dimples which showed failure in a ductile manner.

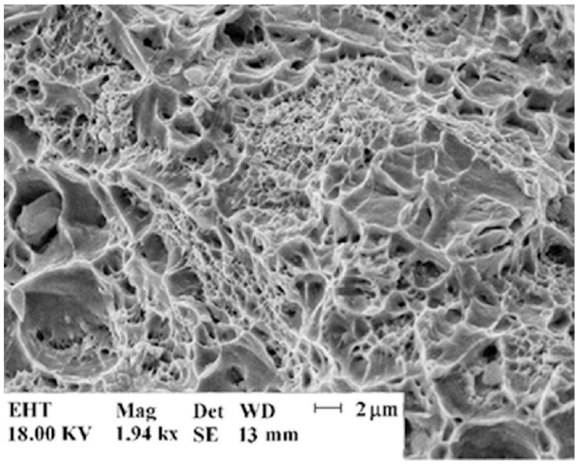

Fig. 4. SEM fractograph of the fractured tensile specimen, ER309L.

In Table 4, the results of Charpy impact test for weld metals at -20 °C and 27 °C are given. The fracture energy amounts of weld metals revealed that the ductile fracture happened to all of them.

Table 4. The average of Charpy V-notch impact energy for the weld metal.

Weld metal type	Impact energy (J) 27 °C	Impact energy (J) -20 °C	Fracture type
ER309L	91	74	Ductile

The scanning electron microscopy micrographs were related to the fracture surface of ER309L (Fig. 5) the weld metals. The images which contained uniform and small dimples showed that the specimens were cracked under the tension pressure in a ductile state, which could be explained in terms of the microstructure of the weld metals and the volume fraction of the austenite [12].

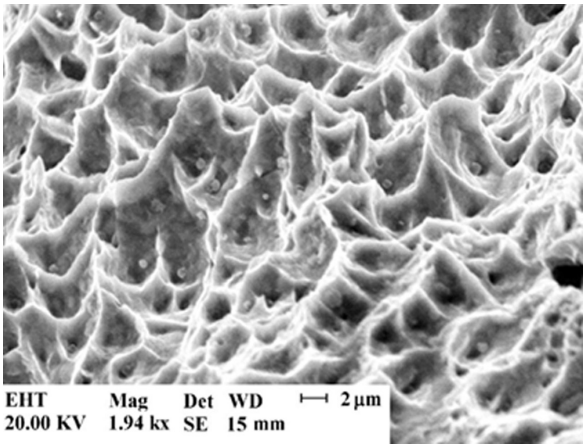

Fig. 5. SEM fractograph of fractured Charpy impact specimen.

The images of the fracture surface of 309L weld metal displayed the characteristics of a ductile fracture. The hardness profile of the specimens welded is displayed in Fig. 6.

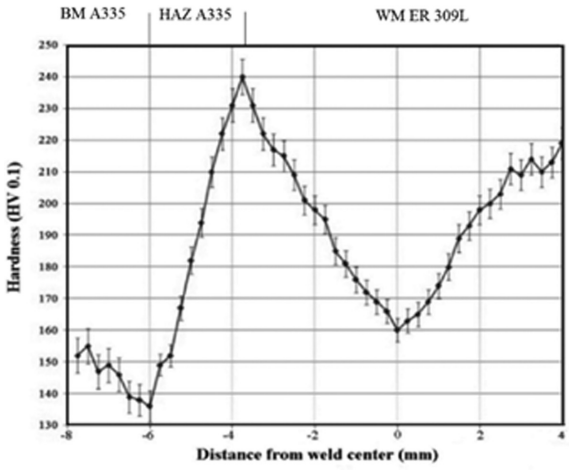

Fig. 6. The hardness profile of dissimilar welding part of A335 low alloy steel with ER309L.

It was revealed that the lowest hardness value was in the central part of the weld zone due to the austenitic structure. The increase in carbon content and the presence of carbides (chromium carbides) near the low alloy steel base metal increased the hardness which resulted from the changes in chemical compositions between A335 steel and the diluted 309L filler metal. Also, a small martensitic zone was formed in the melted boundary, thereby increasing the hardness of this part intensely [9]. The results of EDS line scans are presented in Fig. 7.

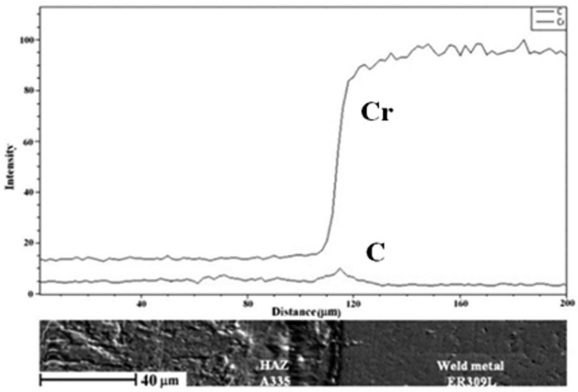

Fig. 7. SEM/EDS line scans image. Redistribution of Cr (blue) and C (red) across the weld interface.

As shown, carbon concentration was decreased in the HAZ of A335 region while there was an increase in carbon concentration in the ER309L weld metal near the fusion line. Also, the amount of chromium between HAZ and weld metal was different [11]. In this figure, it can be seen that the concentration of chromium was decreased from the weld metal to HAZ. This is because of the fact that filler metal ER309L contains higher chromium (23.7%), in comparison to 1.12% in A335 side. A study conducted by Omar and Arivazhagan [10] showed that an increase in hardness across the weld was related to carbon migration from the low alloy steel and carbon steel side towards the austenitic stainless steel.

4. Conclusions

The following conclusions can be drawn from the results:

- The microstructure of the ER309L weld metal included primary ferrite with some austenite at the end of solidification that contained skeleton ferrite.
- In the tensile test, all specimens were broken in the HAZ of A335 low alloy base metal. The welded specimen showed a ductile fracture in impact test and the minimum hardness values of the weldment belonged to ER309L austenitic stainless steel filler metals.
- There was a carbon migration from HAZ to the melt zone in the interface between A335 low alloy steel and 309L filler metal. Also, a tiny martensitic zone was formed in the melt boundary with a high hardness value.

References

[1] J.C. Lippold, D. Koteki: Welding Metallurgy and Weldability of Stainles Steels, John Wiley and Sons,

New Jersey,(2005), 404.
[2] B. Mvola, P. Kah, J. Martikainen: adv. Mater. Sci., 38 (2014), 125.
[3]N. Saeteaw, B. Poopat, I. Phungon, T. Chairuangsri: Aijstpme., 3 (2010), 57.
[4]RL. Klueh, L. King: Weld J., 61 (1982), 302.
[5]L. Falat, M. Svoboda, A.Vyrostkova, I. Petryshynets, M. Sopko: Mater Charact., 72 (2012), 15.
[6] H. Naffakh, M. Shamanian, F. Ashrafizadeh: J Mater Process Technol., 209 (2008), 3628.
[7]M. NourI, A. Abdollah-Zadeh, F. Malek :Mater Sci Technol., 23 (2007), 817.
[8]D.L. Olson: WeldingBrazing Soldering, ASM Handbook, Vol 6, ASM International, Metals Park., (1993), 235.
[9]H.Jang, C. Parkb, H. Kwona: Acta., 50 (2005), 3503.
[10] N. Arivazhagan, S. SurendraSingh: Materials and Design., 23 (2011), 3036.
[11] H. ShahHosseini, M. Shamanian, A. Kermanpur: Materials Characterization., 62 (2011), 425.
[12]H. Muesch: Nucl Eng Des., 2 (2003), 155.